Advances in Reliability, Safety and Security, Part 2 – Kołowrocki, Magryta-Mut (eds.)

Advances in Reliability, Safety and Security

ESREL 2024
Monograph Book Series

Dependence Of UD CFRP Fatigue Life On Interface Shear Strength

Shufeng Zhang[a,b], Guofeng Song[a,b], Fulei Zhu[a,b], Yashun Wang[a,b], Zhengwei Fan[a,b], Xun Chen[a,b]

[a] *Science and Technology on Integrated Logistics Support Laboratory, National University of Defense Technology, Changsha 410073, China*
[b]*College of Intelligence science and technology, National University of Defense Technology, Changsha 410073, China*

Abstract

Accurate estimation on the fatigue life of CFRP is vital for appropriate structure design. The effect of interface shear strength on tension-tension fatigue life of CFRP is investigated in this work. A procedure is developed to calculate the fibre break and interface debond damage caused by fatigue load. 3D FE model with fibre beam element and matrix solid element is employed to determine initial fibre break caused by the first load cycle. CFRP specimens with interface shear strength at 26MPa and 17MPa are tested at different stress ratio and stress amplitude. The predicted fatigue life agrees well with test results, where the CFRP with higher interface shear strength possesses larger fatigue life. The the fatigue life of CFRP with interface shear strength at 26MPa is larger than that of 17MPa, roughly by 1 order of magnitude. Higher interface shear strength helps on slowing interface debonding speed and increasing the debond energy threshold, which contributes to higher fatigue life.

Keywords: fatigue, CFRP, damage accumulation, interface shear strength

1. Introduction

Carbon fibre reinforced plastic (CFRP) is widely used in aircraft, satellites, ships, vehicles and civil structures, due to its superior mechanical strength as well as low density. According to a statistical study by the US National Institute of Standards and Technology, approximately 60% of composite structural failure are related to fatigue(Halford and Manson, 2006). Therefore, accurate estimation on the fatigue life of CFRP is vital for appropriate structure design. CFRP is usually composed of a number of unidirectional plies (lamina) with different orientation, longitudinal failure would trigger macro-scale fiber break and consequently result into ultimate failure. Hence, it is fundamentally important to achieve comprehensive understanding on the fatigue behavior of unidirectional (UD) CFRP.

A number of researchers have studied the fatigue behaviour of CFRP based on mathematical statistics of fatigue test data of CFRP specimens. One approach is to characterize the stiffness degradation trend of specimens(Varvani-Farahani and Shirazi, 2007). The residual stiffness is used to represent fatigue damage accumulation. However, such methodology usually requires a large number of test specimens, and stiffness degradation till structure destruction is sometimes not significant (Brunbauer and Pinter, 2015). Another approach is try to determine the S-N curve based on the fatigue life corresponding a number of different load level, but the S-N curve often shows large uncertainty.

Another approach attempts to predict the fatigue life of CFRP based on the modelling of micro-scale damage accumulation of constituent materials. Zhu et al(Zhu et al., 2021) constructed 2D fatigue life prediction model based on fatigue characteristic of single fiber and expansion of broken fiber clusters, where the fatigue damage of carbon fibre is considered. Fazlali et al developed a UD composite fatigue model that considers fiber breaks and fiber-matrix debond growth(Fazlali et al., 2021). Although current micro-scale damage accumulation seems to over predict the fatigue life of CFRP, it provides a new approach to understand the dependence of CFPR fagitue life on micro-scale factors, which contributes to optimization of manufacture procedure.

This paper studies the dependence fatigue life of UD CFRP on the fibre/matrix interface shear strength (IFSS). A representative model in the form of a cuboid volume of CFRP with fibre aligning the length direction is employed. Fibre is equally divided into a number of small sections along the length direction, and each section is assigned by a fatigue strength sampled from a Weibull distribution. Finite element (FE) model is proposed to determine initial fibre break during the first loading cycle. A damage accumulation model is built to characterize the fatigue process where different IFSS is considered. Fatigue tests of CFRP specimens with different IFSS are carried out, where the test results agrees well with the model prediction.

2. Micro-damage of CFRP during the first load cycle

Due to the uncertainty on the ultimate strength of carbon fibre, a less number of fibre would break at weak points during the first loading cycle. The fibre break consequently results in initial fibre debonding at the fibre fracture position. Such initial fibre break and interface debonding is the starting of the micro-scale damage accumulation.

2.1. Geometric and mesh of FE model

3D FE model is constructed to determine broken fibre during the first loading cycle, where the loading is considered to be applied quasi-statically. The geometrical model based on 3D representative volume element (RVE) is shown in Fig. 1. The RVE is in a cuboid shape, where the length is 1050μm and the cross-section size is 250μm × 250μm. Fibre are aligned in the z-direction and randomly distributed in the x-y plane. Fibre is modeled by beam element with 2 nodes (B31 in Abaqus), and matrix is modelled by solid element with 8 nodes (C3D8 in Abaqus). Fibre elements are embedded in matrix elements. As many reports show that no significant fibre-matrix debonding is observed in static tension test, the fibre and matrix is assumed to be perfectly bonded in the FE model. The matrix is meshed in cuboid shape with a size of 3μm×3μm×3.5μm, the fibre is also meshed by a length of 3.5μm to achieve a good deformation compatibility Periodic boundary conditions are also employed in the FE model. The z-direction tensile strain is applied to the geometrical model, and a small strain increment of 10^{-5} was set to each step to capture early fiber break development.

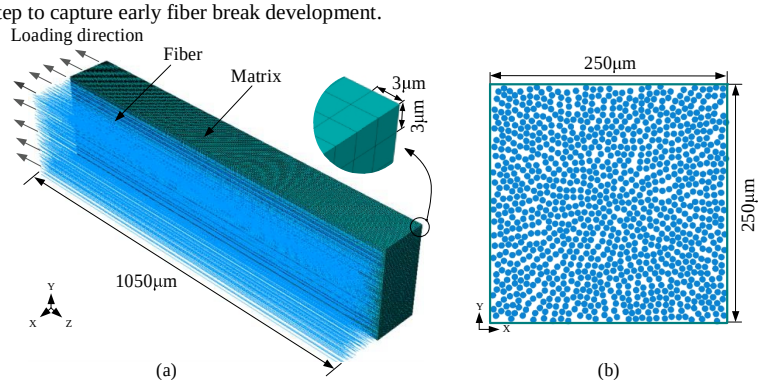

Fig. 1. Geometry, mesh and fiber distribution in FE model (unit in μm).

2.2. Material property of carbon fibre

Carbon fibre strength can be represented by Weibull distribution, written as:

$$P = 1 - \exp\{-(\frac{L}{L_0})^{\alpha_L}(\frac{\sigma_f}{\sigma_0})^{m_L}\} \tag{1}$$

where P is the cumulative failure probability of a fiber at applied tensile stress σ_f., and α_L is a constant value, m_L is the Weibull modulus (shape parameter) of the carbon corresponding to a fiber length at L, and σ_0 is a scale parameter. m_L is written as:

$$m_L = m_0 * (\frac{L}{L_0})^k \tag{2}$$

The parameters σ_0 and m_0 can be obtained by maximum likelihood estimation from tensile test results on fibre samples with length at L_0, which is named as reference gauge length. k is a constant value dependent on fibre mechanical properties, which is determined to be -0.125 from the test data derived in (Naito et al., 2012). A long fibre at length L can be divided by a number of short fibre at length of L^*, and the failure probability of the long fibre can be directly determined using L or indirectly determined using L^* where the smallest strength of the set of short fibre determines the strength of the long fiber, and these two methods should provide identical results on the mean strength of the fibre. Following this rule, α_L can be uniquely determined.

By a number of fibre strength test with a reference gauge length at 25mm, the constants on the statistical distribution of carbon fibre strength corresponding to a gauge length at 3.5μm is shown in Table 1. Then, in the FE model,

Table.1 Fibre properties with gauge length L=3.5μm.

Fibre type	k	α_L	σ_L(MPa)	m_L	L (μm)
T700	-0.125	0.91	7014.4	14.91	3.5

Based on the Timoshenko beam element (B31) with 2 nodes, a new constitutive model is developed with progressive damage for the fibre beam element, which is implemented by user-mat subroutine in commercially available software ABAQUS2022. The developed constitutive model with damage evolution is shown in Fig .2, inspired by the progressive damage definition in (Zhang et al., 2005). In Fig.3, E_f^0 is the Young's modulus of the fiber, σ_f^s is the tensile strength, ε_f^s is the failure strain corresponding to the tensile strength. If the element strain is smaller than ε_f^s, the element tensile stress is updated by:

$$\sigma_i = \sigma_{i-1} + E_f^0 * \Delta\varepsilon \tag{3}$$

where σ_i is the fibre element stress in the i-th step, and $\Delta\varepsilon$ is the strain increment. If fiber element strain beyond ε_f^s, fibre modulus is reduced, expressed as:

$$E_f(i+1) = \alpha * E_f^0 \tag{4}$$

where α is the modulus reduction factor.

The stress increment in the fiber element is then calculated as:

$$\Delta\sigma_f(i+1) = E(i+1) * \Delta\varepsilon - \beta * \sigma_f(i) \tag{5}$$

where β is a tensile stress reduction factor. The fibre stress is then updated by:

$$\sigma_f(i+1) = \sigma_f(i) + \Delta\sigma_f(i+1) \tag{6}$$

As the strain increases, the damage continues to accumulate, and the modulus and stress of the fibre element gradually decrease until they approach to zero. Therefore, the progressive damage process of fiber element can be controlled by setting the modulus reduction factor α and the stress reduction factor β. In this work, α is usually a small value, and β should be between 0 and 1. In this work α is set to be 0.001, and β is set to be 0.6 considering good calculation convergence.

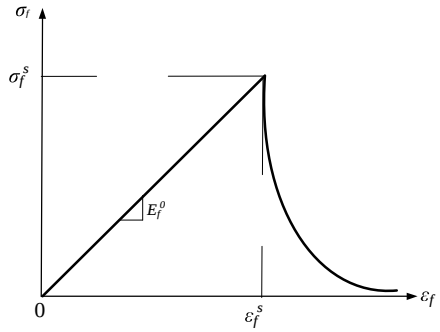

Fig.2. Constitutive model of cabon fiber.

2.3. Material property of matrix

In this study, epoxy resin 736LT is selected as the matrix material for T700 carbon fibre. Epoxy resin has been experimentally shown to be elastic–plastic and brittle, and its constitutive model is schematically shown in Fig.3. The plastic yielding process of the matrix can be represented by the extended Drucker-Prager criterion [36]:

$$F = t - p\tan\xi - d = 0 \tag{7}$$

$$t = \frac{q}{2}[1 + \frac{1}{\kappa} - (1 - \frac{1}{\kappa})(\frac{\chi}{q})^{} \tag{8}$$

where p is hydrostatic pressure, q is Mises equivalent stress, χ is the third invariant of deviator stress, ξ is the internal friction angle, d is cohesion of the material, κ is the ratio of triaxial tensile yield stress to triaxial compressive yield stress. Furtherly, parameter D is used to describe the development of damage(Yang et al., 2014, Yang et al., 2012), which is expressed as:

$$D = \frac{L\varepsilon_m^{\ p}}{u_m^{\ f}} = \frac{u_m^{\ p}}{u_m^{\ f}} \tag{9}$$

where L is the characteristic length of model, ε_m^p and u_m^p represent the equivalent plastic strain and displacement, and u_m^f is the equivalent plastic at failure. Before damage initiation, $u_m^p = 0$; after damage initiation, $u_m^p = L\varepsilon_m^p$. Breite et al.(Breite et al., 2022) conducted compression and tensile tests on epoxy materials, and the detailed parameters derived from test results are shown in Table. 2.

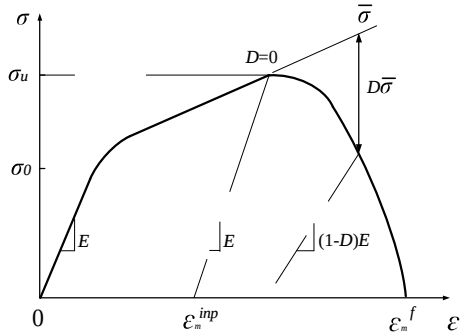

Fig.3. Constitutive model of matrix.

Table. 2. Matrix properties used in FE model (Breite et al., 2022).

Material properties	736LT
Young's modulus, E (GPa)	3150
Poisson's ratio μ_m	0.39
ratio of the yield stress in triaxial tension to compression κ	0.78
Internal friction angle ξ	24°
Tensile equivalent plastic strain ε_t	0.035
Tensile strength σ_u	101.6
Stress triaxiality for uniaxial tension η_t	-1/3
Compressive equivalent plastic strain ε_c	0.51
Compressive strength σ_c (MPa)	107.8
Stress triaxiality for uniaxial compression η_c	1/3
Fracture energy G_{max} (J/m^2)	0.5

2.4. Fibre breakage development

The derived stress-strain curve by the FE model is shown in Fig. 4. It is clearly seen that the stress increases linearly as the strain increment till sudden fracture, which agrees with most experimental observation. Fig.5 shows the development of fibre breakage at different stress level. It is seen that a tensile strain at 1.5% causes several fibre breakage at random positions. The fibre break points increases heavily after the ultimate load arrived. By such approach, the initial fibre break due to the first cycle load can be determined, and it depends on the peak load of the first loading cycle.

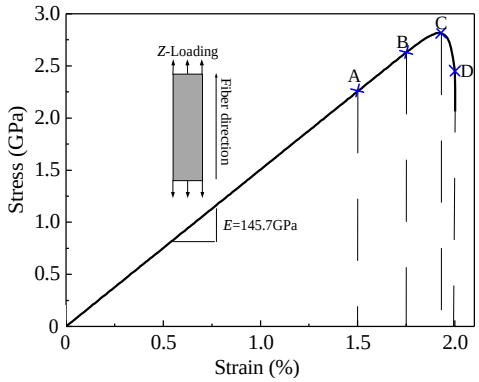

Fig.4. Representative stress-strain curve of T700 composite obtained from the FE model.

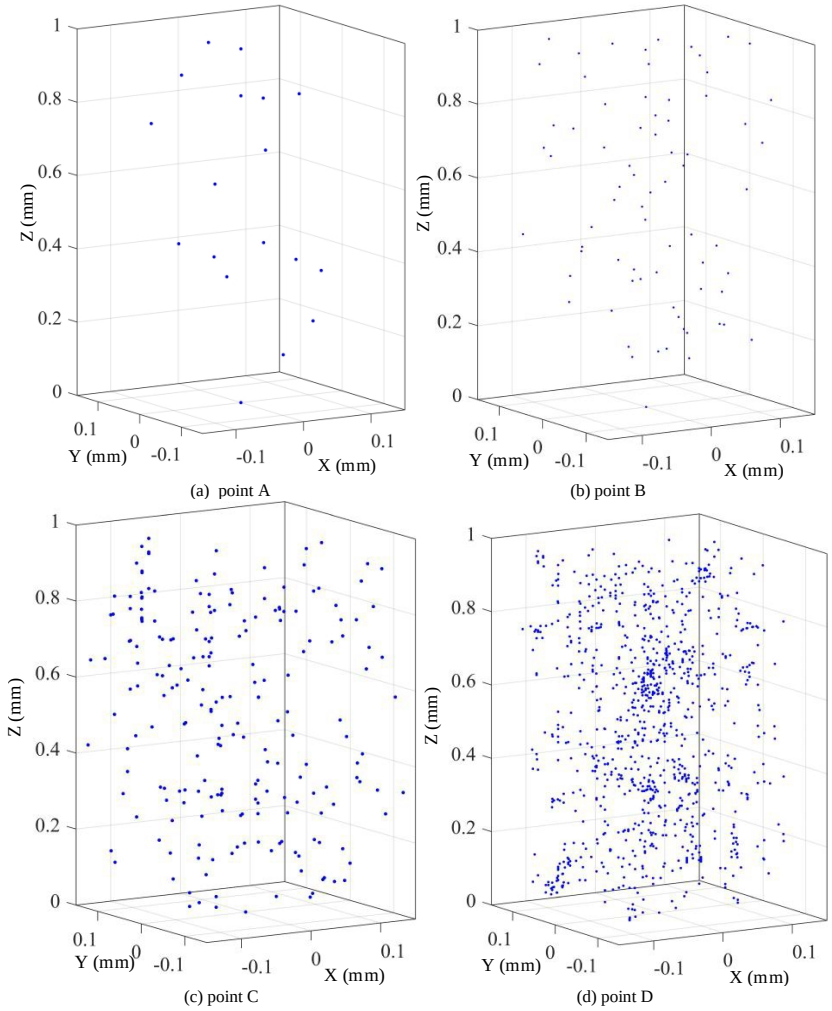

Fig.5. The spatial distribution of the broken fibers in RVE derived from FE model at corresponding loading points A, B, C and D in Fig. 4.

3. Modelling on accumulation of fatigue damage

3.1. Fibre fatigue mechanism

The S-N curve of T700 carbon fibre is experimentally obtained at a stress ration (R) at 0.2(Bunsell and Somer, 1992), and the S-N curve is expressed as:

$$\lg \sigma_{\max} = -0.013 \lg N_f + 2.95 \tag{10}$$

where $\sigma_{\max}$ is the peak load, and N_f is the number of cycles. $\sigma_{\max}$ is also named as the fatigue strength corresponding to a loading cycle number at N_f . Considering the uncertainty of the fatigue strength, the fatigue strength is considered to follow the same Weibull distribution as the static strength. The distribution of fatigue strength is expressed as:

$$P(\sigma) = 1 - \exp\{-(\frac{L}{L_0})^{\alpha_L} (\frac{\sigma_{\max}}{\sigma_0})^{m_L}\} \tag{11}$$

Employing Palmgren-Miner inear fatigue cumulative damage theory, the damage accumulation (D) of single fiber is calculated as:

$$D = \sum_i \frac{n_i}{N_f(\sigma_{\max})} \tag{12}$$

where $N_f(\sigma_{\max})$ is the fatigue life corresponding to peak stress of cyclic load at $\sigma_{\max}$, and n_i is the number of fatigue cycles. $D = 1$ indicates the fatigue failure of fiber. It is important to notice that Eq.(10) –(12) can be converted into damage accumulation formula at different stress ratio using the Goodman equation.

3.2. Interface debonding growth mechanism

Interface debonding is an important micro-scale damage during the fatigue process of CFRP. After initial debonding is generated at the fibre break position, the debonding length grows due to the cyclic shear stress at the interface. Paris-Erdogan law(Swolfs et al., 2015) is employed to describe the debonding length growth as the increase of loading cycles, which is expressed as:

$$\frac{dl_d}{dN} = C(\Delta G_{\text{II}} - (\Delta G_{\text{II}})_{th})^n \quad \Delta G_{\text{II}} > (\Delta G_{\text{II}})_{th} \tag{13}$$

where l_d is the debonding length, N is the number of load cycles, ΔG_{II} is energe release rate in a loading cycle, and $(\Delta G_{\text{II}})_{\text{th}}$ is the critial energe release rate of the interface. C and n are constants which can be fitted by experimental data. $(\Delta G_{\text{II}})_{\text{th}}$ can be determined by static fibre pull-out test. ΔG_{II}depends on the fatige stress amplitude, stress ratio and current debonding length. Negelecting the thermal effect, the ΔG_{II} is expressed as:

$$\Delta G_{\text{II}} = k_d \frac{E_f r_f}{4} \frac{E_m}{E_c} (\sigma_{f-\max} - \sigma_{f-\min}) \tag{14}$$

where E_f is the Young's modulus of fibre, E_m is the modulus of matrix, E_c is the Young's modulus of composite, r_f is the radius of fibre. $\sigma_{f\text{-max}}$ and $\sigma_{f\text{-min}}$ are the maximum and minmum tensile stress of fibre during a loading cycle. k_d is a constant related to the debonding length(Fazlali et al., 2021). As CFRP with higher interface shear strength would has a higher $(\Delta G_{\text{II}})_{\text{th}}$, less interface debond would be generated during the fatigue loading process.

3.3. Procedure of fatigue life prediction

The schematic illustration of damage development of UD CFRP bearing tension-tension fatigue load is shown in Fig.6. Firstly, fibre breaks at weak points, and it results into initial interface debonding. As the increase of loading cycles, the interface debonding grows and new fibre breaking occurs. Finally, macro-scale fatigue fracture occurs due to a large number of fibre breaking.

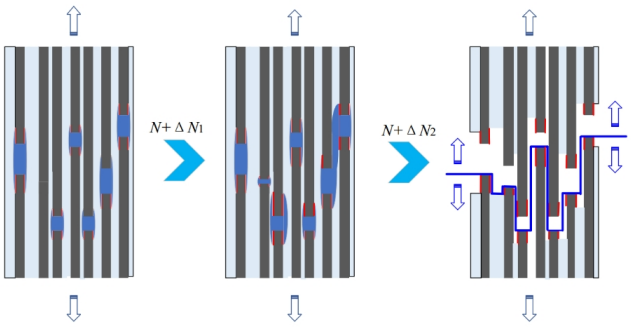

Fig. 6. Schematic illustration of damage development in the fatigue loading process.

According the micro-scale damage accumulation mechanism, the proposed procedure of fatigue life prediction is shown in Fig. 7, which is developed based on reference(Fazlali et al., 2021). The prediction procedure includes following steps:

Step 1: Build 3D RVE model with random fibre distribution, the probabilistic distribution of fibre static and fatigue strength is set.

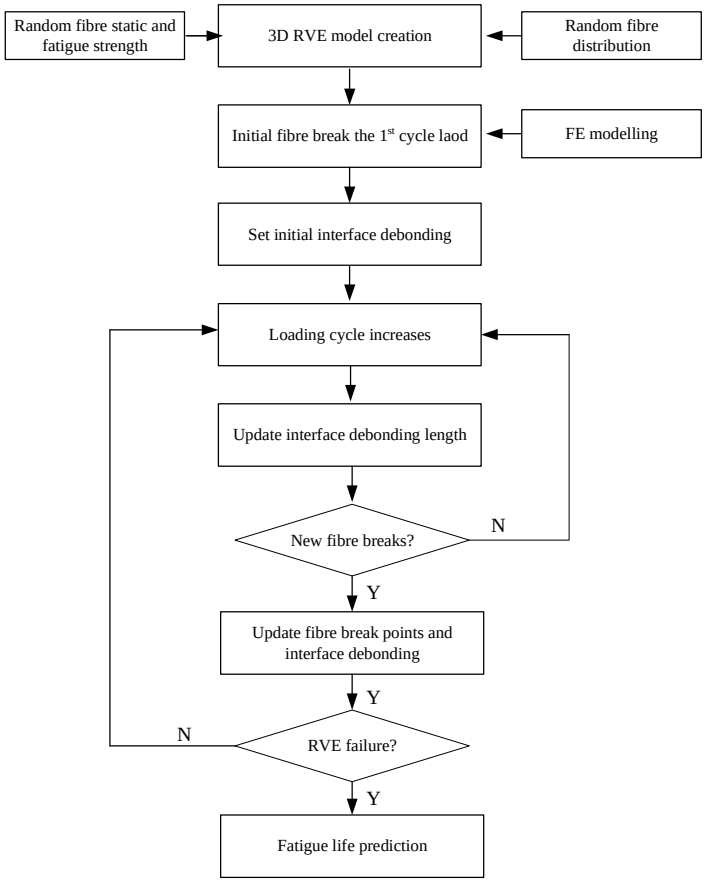

Fig. 7. Procedure of fatigue life calculation of CFRP fatigue life.

Step 2: FE model is built to derive initial fibre break using the methodology introduced in Section 2.

Step 3: The initial interface debonding length at the position of fibre break points is set. Normally, shorter initial interface debonding length is set for CFRP with higher interface shear strength.

Step 4: Increase loading cycles.

Step 5: Update interface deboning length according to Section 3.2. The stress distribution is correspondingly re-calculated.

Step 6: Judge if new fibre breaking occurs according to Section 3.1. If there is no new fibre breaking, return to Step 4; otherwise, go to Step 7.

Step 6: Judge if the RVE fails. The RVE failure could be determined by a threshold on the number of broken fibres or stiffness degradation. If RVE does not fail, return to Step 4; otherwise, the procedure stops.

4. Prediction of CFRP fatigue life and experimental verification

Fatigue life of CFRP with two different IFSS is investigated. 2 types of CFRP are prepared with different sizing agent on carbon fibre interface. The IFSS was expeimentally derived by a micro-drop test, as a benchmark to conduct the fatigue life prediction. The IFSS of the two different specimens were obtained as 17MPa and 26MPa, respectively. The critial energe release rate $(\Delta G_{II})_{th}$ was also determined from the maximum load value from the micro-drop test. For convinience, CFRP with IFSS at 26MPa is shorten by strong CFRP, and the CFRP with IFSS at 17MPa is shorten by weak CFRP.

4.1. Fatigue life prediction of CFRP with different IFSS

Fatigue life of CFRP with different IFSS (17MPa, 20MPa, 23MPa, 26MPa) is predicted using the procedure introduced in Section 3.3. Fig.8 shows the development of fibre breaking as the increase of loading cycles. It is clearly seen that the CFRP with weaker IFSS generates more fibre breaking points corresponding to the same loading cycle. As sharp increase of fibre breaking usually results to fatigue fracture, it also tells that CFRP with higher IFSS have a larger fatigue life. It is seen that the fatigue life of CFRP with IFSS at 26MPa is larger than that of CFRP with IFSS at 17MPa, roughly by 1 order of magnitude (see mark position of A, B, C ,D).

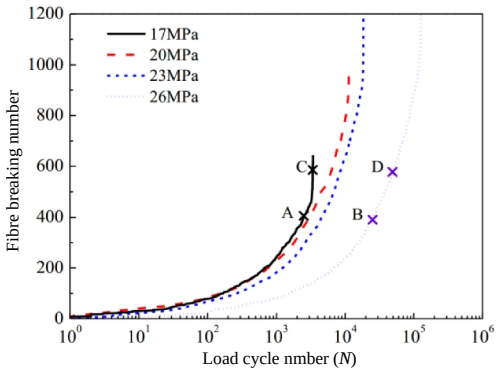

Fig.8. Fibre breaking development as the increase of loading cycle.

4.2. Fatigue life test of CFRP with different IFSS

CFPR specimens are prepared with two different IFSS, which are 26MPa and 17MPa respectively. The ultimate tensile strength (UTS) of two types specimens is firstly tested by 10 specimens for each type. The UTS of strong interface specimen and weak interface specimen are tested to be 2.73GPa and 2.38GPa, respectively. Then, hydraulic test machine MTS370 was employed to conduct the fatigue test. The lading cycle is in sinusoidal shape, and the loading frequency is 10Hz. Load control mode is employed to ensure identical stress amplitude for all cycles. An extensometer is fixted on specimens to monitor specimen strain. Before the cyclic loading, the specimen is firstly loaded to the stress-peak, by a quasi-static loading speed. The fatigue test was conducted at several different stress levels (0.6, 0.7, 0.8, 0.8, 0.9) and stress ratios (0.1, 0.7). The fatigue test was finished if specimen fracture occurred or the load cycle number reached to 1×106, which is considered to be a fatigue limit.

The test results on fatigue life of all specimens at different stress levels and stress ratios are listed in Table 3. It is seen that the fatigue life is heavily dependent on interface strength, stress ratio and stress level. Generally, the fatigue life reduces as the increase of stress level and decrease of stress ratio, which is as expected. Importantly, it

is seen that the fatigue life of CFRP with IFSS at 26MPa is obviously larger than that of IFSS at 17MPa, approximately by 1 order of magnitude. Such influence of IFSS on fatigue life agrees well with numerical modelling.

Table 3. Test results on fatigue life of CFRP specimens.

Specimen type	Stress ratio	Stress level	Valid specimen number	Average fatigue life
Strong interface *IFSS*=26MPa	0.1	0.6UTS_s	3	115181
		0.7 UTS_s	5	7684
		0.8 UTS_s	5	1213
		0.9 UTS_s	5	154
	0.7	0.6 UTS_s	3	$>10^6$
		0.7 UTS_s	5	53939
		0.8 UTS_s	5	18041
		0.9 UTS_s	5	558
Weak interface *IFSS*=17MPa	0.1	0.6 UTS_w	3	22596
		0.7 UTS_w	5	3665
		0.8 UTS_w	5	936
		0.9 UTS_w	3	268
	0.7	0.6 UTS_w	3	24293
		0.7 UTS_w	5	4770
		0.8 UTS_w	5	1314
		0.9 UTS_w	5	211

UTS_s=2.73GPa, UTS_w=2.38GPa

5. Conclusion

The effect of interface shear strength on the tension-tension fatigue life of CFRP is investigated. A procedure is developed to calculate the fibre break and interface debond damage caused by fatigue load. 3D FE model with fibre beam element and matrix solid element is employed to determine the initial fibre break caused by the first load cycle. CFRP specimens with interface shear strength at 26MPa and 17MPa are tested at different stress ratio and stress amplitude. The predicted fatigue life agrees well with test results, where the CFRP with higher interface shear strength possesses larger fatigue life. The the fatigue life of CFRP with IFSS at 26MPa is larger than that of CFRP with IFSS at 17MPa, roughly by 1 order of magnitude. Higher interface shear strength helps on increasing the debond energy threshold and slowing interface debonding speed and, which contributes to higher fatigue life.

Acknowledgements

This work is supported by the National Natural Science Foundation of China (Grant No. 11991032, 51975577,11872371), and the science and technology innovation Program of Hunan Province(2020RC4022).

References

Breite, C., Melnikov, A., Turon, A., et al. 2022. Detailed experimental validation and benchmarking of six models for longitudinal tensile failure of unidirectional composites. Composite Structures, 279**,** 114828.

Brunbauer, J., Pinter, G. 2015. Fatigue life prediction of carbon fibre reinforced laminates by using cycle-dependent classical laminate theory. Composites Part B: Engineering, 70**,** 167-174.

Bunsell, A. R., Somer, A. M. 1992. The tensile and fatigue behaviour of carbon fibres. 18**,** 263-267.

Fazlali, B., Lomov, S. V. & Swolfs, Y. 2021. Fiber break model for tension-tension fatigue of unidirectional composites. Composites Part B: Engineering, 220**,** 108970.

Halford, G. R., Manson, S. S. 2006. Fatigue and Durability of Structural Materials, ASM International.

Naito, K., Yang, J.-M., Tanaka, Y., et al. 2012. The effect of gauge length on tensile strength and Weibull modulus of polyacrylonitrile (PAN)- and pitch-based carbon fibers. Journal of Materials Science, 47**,** 632-642.

Swolfs, Y., Mcmeeking, R. M., Verpoest, I., et al. 2015. The effect of fibre dispersion on initial failure strain and cluster development in unidirectional carbon/glass hybrid composites. Composites Part A: Applied Science and Manufacturing, 69**,** 279-287.

Varvani-Farahani, A., Shirazi, A. 2007. A Fatigue Damage Model for (0/90) FRP Composites based on Stiffness Degradation of 0° and 90° Composite Plies. Journal of Reinforced Plastics and Composites, 26**,** 1319-1336.

Yang, L., Wu, Z., Cao, Y., et al. 2014. Micromechanical modelling and simulation of unidirectional fibre-reinforced composite under shear loading. Journal of Reinforced Plastics and Composites, 34**,** 72-83.

Yang, L., Yan, Y., Liu, Y., et al. 2012. Microscopic failure mechanisms of fiber-reinforced polymer composites under transverse tension and compression. Composites Science and Technology, 72**,** 1818-1825.

Zhang, Y., Xia, Z. Ellyin, F. 2005. Nonlinear viscoelastic micromechanical analysis of fibre-reinforced polymer laminates with damage evolution. International Journal of Solids and Structures, 42**,** 591-604.

Zhu, F., Zhang, S., Yu, D., et al. 2021. Fiber break evolution and fatigue life prediction of CFRP with random fiber distribution. Composite Structures, 259**,** 113475.